CAROE, G. M. (1978). *William Henry Bragg* 1862-1942: *Man and Scientist.* Cambridge Univ. Press.
CORK, J. M. (1927). *Philos. Mag.* pp. 688-698.
FRIEDRICH, W., KNIPPING, P. & LAUE, M. (1912). *Interferenz-Erscheinungen bei Röntgenstrahlen.* In *Sitzungsber. Kgl. Bayer: Akad. Wiss.* pp. 303-322.
HAVIGHURST, R. J. (1927). *Phys. Rev.* **29**, 1-12.
KUHN, T. S. (1970) *The Structure of Scientific Revolutions.* Univ. of Chicago Press.
MEDAWAR, B. P. (1979). *Advice to a Young Scientist.* New York: Harper & Row.
PHILLIPS, SIR DAVID (1979). *William Lawrence Bragg,* 31 *March* 1890-1 *July* 1971. *Biographical Memoirs of Fellows of the Royal Society,* **25**, 75-143.

Acta Cryst. (1990). A**46**, 643-649

Investigation of Surface-Layer Structure of Single Crystals with Triple-Crystal X-ray Diffractometry

BY A. YU. KAZIMIROV AND M. V. KOVALCHUK

Institute of Crystallography of the Academy of Sciences of the USSR, Leninsky Prospekt 59, *Moscow* 117333, *USSR*

AND V. G. KOHN

I. V. Kurchatov Institute of Atomic Energy, Kurchatov Square 46, *Moscow* 123182, *USSR*

(*Received* 1 *June* 1989; *accepted* 22 *January* 1990)

Abstract

The possibilities of the X-ray triple-crystal diffractometry (TCD) method in studying the tails of rocking curves of both a perfect crystal and a crystal with a disturbed surface layer are shown. It was found that at large deviation angles (α) from the Bragg condition the pseudopeak of the TCD curves significantly exceeds the main peak. The thermal diffuse scattering in the monochromator crystal is discussed as one of the reasons for this effect. This phenomenon is also responsible for the violation of the $I(\alpha) \propto 1/\alpha^2$ dependence in double-crystal diffractometry (DCD). By measuring the intensities of the main peaks of TCD curves, it is possible to separate the diffuse and the coherent scattering components in the rocking curves obtained by DCD.

1. Introduction

Much attention has been paid in the last few years to the study of surface-layer structures by X-ray diffraction. It is well known that the shape of a rocking curve (RC) of a crystal with a disturbed surface layer changes with respect to that of an ideal crystal, due to the depth distribution of the lattice strain $\Delta d/d$ and the atomic disorder in the layer.

Several methods have been developed to fit the experimental rocking curves. For example, the method of computing directly the RC by the Takagi-Taupin equations (Burgeat & Taupin, 1968; Fukuhara & Takano, 1977), the method of integral characteristics (Afanasev, Kovalchuk, Kovev & Kohn, 1977; Kohn, Kovalchuk, Imamov & Lobanovich, 1981) and the methods based on the kinematical theory of X-ray diffraction (Kyutt, Petrashen & Sorokin, 1980; Speriosu, Glass & Kobayashi, 1979; Kohn, Prilepsky & Sukhodreva, 1984) are noteworthy. All these methods deal with the analysis of the angular dependence of the coherent-scattering components. However, most of the RC measurements are carried out by a double-crystal diffractometer arranged in the parallel non-dispersive $(n, -n)$ setting, in which all the intensity scattered by the sample is collected. This intensity contains not only a coherent contribution but also a diffuse scattering, which modifies the RC shape. As will be shown by an example relating to the study of a surface-implanted layer, this effect can lead to either a distortion or an entire loss of information about the surface-layer structure. The study of samples with surface layers containing a lot of defects can be carried out effectively by the method of triple-crystal X-ray diffractometry (TCD). This method makes possible the separation of the coherent and diffuse contributions by analysis of the angular intensity distribution with the help of the third crystal (analyzer). Successfully used by Iida & Kohra (1979), the TCD method has been widely applied lately (for example, by Afanasev, Aleksandrov, Imamov, Lomov & Zavyalova, 1984; Cembali, Servidori, Solmi, Sourek, Winter & Zaumseil, 1986; Zaumseil, Winter, Cembali, Servidori & Sourek, 1987). Of course, the TCD method is more complicated and difficult in comparison with the double-crystal X-ray diffractometry (DCD) method. It is necessary to measure the entire TCD curve or, at least, the integral intensity of the main peak of this curve to obtain only one

0108-7673/90/080643-07$03.00

experimental point for the RC. Also, for the practical realization of this method, more complicated multicrystal diffractometers are necessary. Nevertheless, when there is strong diffuse scattering in a sample, this approach is the only correct one. Moreover, even in the absence of diffuse scattering from the crystal defects, as will be shown below by the analysis of a rather wide angular region of the RC of a perfect crystal, the tails of the RC contain additional intensity due to thermal diffuse scattering (TDS) from the monochromator crystal. In both cases (diffuse scattering from the defects and TDS), the analysis of the DCD RC by the theory of coherent X-ray scattering can lead to significant mistakes (for example, to the wrong deformation profiles obtained by computer simulation).

The purpose of the present work is a qualitative comparison of the DCD and TCD methods in the analysis of the surface-layer structures of single crystals. The physical reasons for some peculiarities observed in experimental rocking curves are also given.

In the next section, the comparative analysis of the experimental rocking curves of a single crystal, obtained by double- and triple-crystal diffractometry methods, is given. In § 3 the role of the thermal diffuse scattering from the monochromator crystal is discussed and its contribution to the intensity of the pseudopeak of the spectrum is calculated. The results of the separate measurement of the coherent part of the RC, in the presence of a strong diffuse scattering from the sample, are presented in § 4.

2. Tails of the rocking curves of single crystals

The angular dependence of the X-ray intensity scattered from a perfect silicon crystal has been measured by a double-crystal nondispersive $(n, -n)$ parallel setting with a symmetrical monochromator crystal. Fig. 1(*a*) (the upper curve) shows the intensity of the reflected beam normalized to the intensity of the incident beam (DCD rocking curve). We used the 400 reflection of Mo $K\alpha$ radiation of a conventional X-ray tube. As is already known (Pinsker, 1978), the tails of the rocking curve of a single crystal can be described by

$$P_R^{\mathrm{coh}}(\alpha)=\left(\frac{\lambda r_0|F_h|}{VhC}\right)^{1/2}\frac{K\beta}{\alpha^2}. \qquad (1)$$

The intensity decreases as $1/\alpha^2$ with increasing angle α (deviation from the exact Bragg position for a reflected beam). In (1), λ is the wavelength, $r_0 = e^2/mc^2$ is the classical electron radius, F_h is the structure factor. For silicon, $F_h = 8f_h \exp(-M_h)$, where f_h is the atomic scattering factor and $\exp(-M_h)$ is the Debye–Waller factor, h is the modulus of the reciprocal-lattice vector, V is the volume of a unit cell, $C = \cos\theta_b$, θ_b is the Bragg angle, $K = (1+C_2^2)/(1+C_2)$ is the polarization factor, $C_2 = \cos 2\theta_b$, $\beta = \sin(\theta_b - \tau)/\sin(\theta_b + \tau)$ is the asymmetry factor and τ is the angle between the reflecting planes and the crystal surface. The theoretical curve is shown as the lower curve in Fig. 1(*a*). One can see that the experimental curve decreases more slowly than $1/\alpha^2$, and that the ratio of the experimental curve to the theoretical one increases with increasing α. Such a pecularity of the double-crystal rocking-curve tails was observed earlier (Cembali, Servidori, Gabilli & Lotti, 1985; Zaumseil, 1985) but the reason for this effect has not been discussed.

Meanwhile, the reason for this phenomenon can be determined experimentally by the analysis of the TCD curves of a perfect crystal with the increase of the angle α. We recall that a TCD curve of an ideal crystal consists of two peaks. The first is a main peak corresponding to such a position of the crystals ($\Delta\theta = 2\alpha$ in a symmetrical case, $\Delta\theta$ being the deviation of

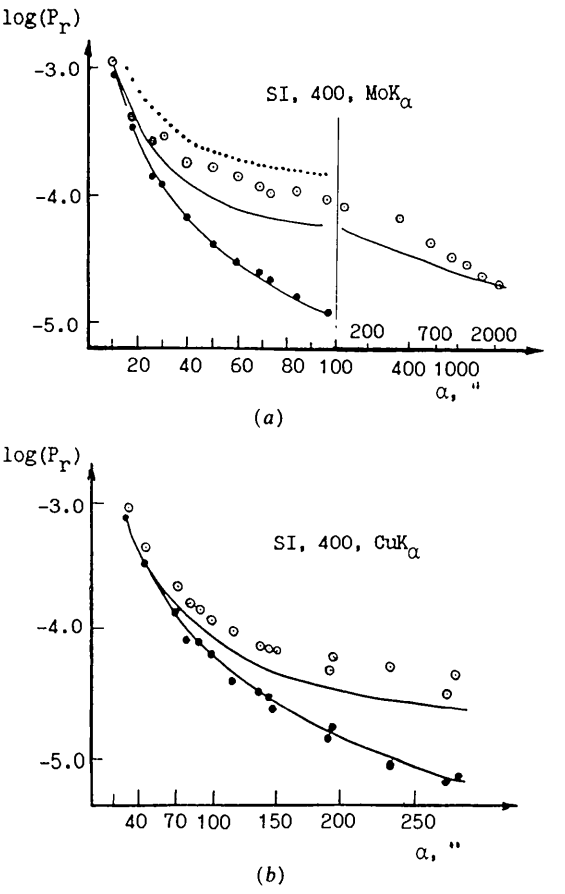

Fig. 1. (*a*) Experimental angular dependences of the pseudopeak (open circles) and the main peak (filled circles) and corresponding theoretical curves (solid lines) for the 400 reflection with Mo $K\alpha$ radiation of a perfect Si crystal. Upper and lower theoretical curves were calculated using (11) and (1), respectively. The experimental DCD curve is shown by a dotted line. (*b*) The same curves for Cu $K\alpha$ radiation (the DCD curve is not shown).

the analyzer crystal from the Bragg position) that total X-ray reflection occurs for the monochromator and the analyzer crystals. The sample reflects the X-rays weakly, since the Bragg condition is not satisfied for large values of α. The second is a pseudopeak, observed at such a position of the analyzer ($\Delta\theta = \alpha$) that the analyzer and the sample reflect the X-rays strongly but the monochromator crystal reflects them weakly. In the first case, (1) corresponds to the sample, in the second case it corresponds to the monochromator. We note that in the second case the direction of the plane wave coming from the first crystal is determined by the positions of the following two crystals. When the sample contains defects, besides the coherent peaks, a diffuse maximum is also observed in the TCD curves.

Typical TCD curves for the 400 reflection of Mo $K\alpha$ radiation are shown in Fig. 2 for different values of α. One can see that at $\alpha = 10''$ the intensities of the pseudopeak and the main peak are approximately equal to each other. With increasing α, the pseudopeak begins to exceed the main peak and at $\alpha = 100''$ the pseudopeak is more intense by about one order of magnitude. We observed the pseudopeak clearly even at $\alpha = 5°$. The result does not change with the mutual replacement of the first and second crystals. We note that diffuse peaks have not been observed in the TCD curves. The α dependences of the integral intensity of the main peak and the pseudopeak for the 400 diffraction of Si with Mo $K\alpha$ radiation are also shown in Fig. 1(a). One can see that the main peak follows (1) perfectly. On the contrary, the angular dependence of the pseudopeak is close to the double-crystal experimental rocking curve.

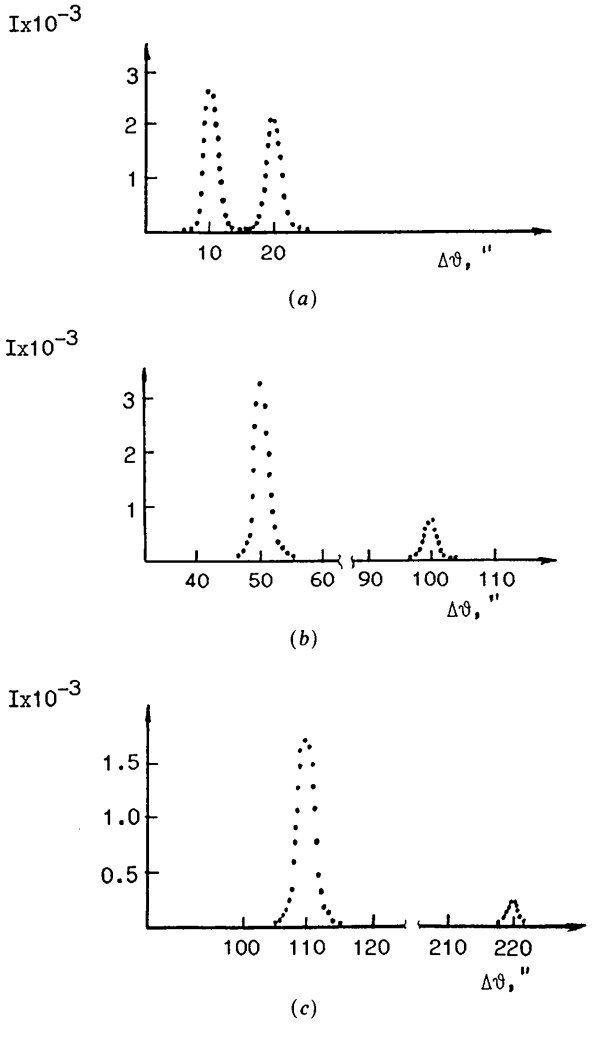

Fig. 2. TCD curves of a perfect Si crystal (400 reflection, Mo $K\alpha$ radiation) for various values of α: (a) $\alpha = 10$; (b) $\alpha = 50$; (c) $\alpha = 110''$. I in counts s^{-1}.

The analogous α dependences for the 400 diffraction with Cu $K\alpha$ radiation are shown in Fig. 1(b). Although the anomalous behavior of the pseudopeak is not so marked as in the previous case, nevertheless, by $\alpha = 200''$ the pseudopeak is five times higher than the main peak.

Therefore, the deviation of the experimental tails of a DCD rocking curve from the theoretical ones can be connected to the anomalous angular dependences of the pseudopeak intensity in the TCD curves.

3. Contribution of the thermal diffuse scattering from the monochromator crystal to the intensity of the pseudopeak

As already noted above, in order to consider theoretically the RC tails, it is necessary to take into account not only the coherent but also the thermal diffuse scattering (TDS). In the angular region of the main peak, the TDS is extremely small, since only few phonons with wave vectors **q** perpendiuclar to the crystal surface take part in it. Phonons with other **q** directions contribute to the TCD curve at different values of the scanning angle $\Delta\theta$, but this contribution is also small.

On the other hand, the radiation incident on the first crystal has a rather high intensity in a wide angular range. It is possible to rescatter by TDS all incident X-rays into the plane wave with direction determined by subsequent crystals. In other words, a photon incident on the first crystal at an arbitrary angle could be scattered on a phonon so that the resulting plane wave would correspond to the angular region of the pseudopeak.

The situation is illustrated in Fig. 3, where the cross section of a crystal on the scattering plane is shown. The x axis is directed along the surface, the z axis is directed along the outward normal. In the general case of asymmetrical scattering, the reciprocal-lattice vector **h** makes an angle τ with the z axis. The wave vector **k** of the plane wave incident on the

monochromator crystal can be represented as $\mathbf{k}=\mathbf{k}_0+\mathbf{\Delta}_0$, where $\mathbf{k}_0$ satisfies exactly the Bragg condition $k_0^2=k_h^2$, $\mathbf{k}_h=\mathbf{k}_0+\mathbf{h}$. The vector $\mathbf{\Delta}_0$ is perpendicular to $\mathbf{k}_0$ and its Cartesian coordinates are

$$\begin{aligned}\Delta_{0x}&=-\kappa\alpha_0\sin(\theta_b-\tau), \quad \Delta_{0y}=-\kappa\varphi_0,\\ \Delta_{0z}&=-\kappa\alpha_0\cos(\theta_b-\tau), \quad \kappa=2\pi/\lambda,\end{aligned} \tag{2}$$

where α_0 is the angle in the scattering plane and φ_0 is the angle in the plane normal to it.

The wave vector of a scattered wave is $\mathbf{k}'=\mathbf{k}_h'+\mathbf{\Delta}_h$ and the coordinates of $\mathbf{\Delta}_h$ are

$$\begin{aligned}&\Delta_{hx}=-\kappa\alpha\sin(\theta_b+\tau), \Delta_{hy}=0,\\ &\Delta_{hz}=\kappa\alpha\cos(\theta_b+\tau).\end{aligned} \tag{3}$$

Fig. 3 shows the vectors $\mathbf{k}_0$, $\mathbf{k}_h$, $\mathbf{\Delta}_h$ and the projection of $\mathbf{\Delta}_0$ on the scattering plane. The vector $\mathbf{h}$ and the angle τ are also shown. In the case of coherent scattering the vectors $\mathbf{\Delta}_0$ and $\mathbf{\Delta}_h$ can differ only in their z components. Therefore, the diffracted wave corresponding to the angle α is formed from the incident wave at $\varphi_0=0$ and $\alpha_0=\alpha/\beta$.

Besides that, a crystal can emit diffuse waves as a result of the scattering of the incident waves with arbitrary values of φ_0 and α_0 on phonons with wave vectors $\mathbf{q}=\mathbf{\Delta}_h-\mathbf{\Delta}_0$. One can obtain a differential reflection coefficient corresponding to these waves following Afanasev, Kagan & Chukhovskii (1968). If α and $\alpha_0\gg\lambda^2 r_0|F_h|/\pi V$, then

$$\frac{\partial^2 P_R^{\mathrm{TDS}}(\alpha)}{\partial\alpha_0\partial\varphi_0}=\frac{\hbar K}{2\mu_0\rho}\frac{\beta}{(1+\beta)}\times\left(\frac{r_0 h|F_h|}{V}\right)^2\sum\frac{n_{q\lambda}}{\omega_{q\lambda}}|\boldsymbol{\eta}\mathbf{V}_\lambda|^2. \tag{4}$$

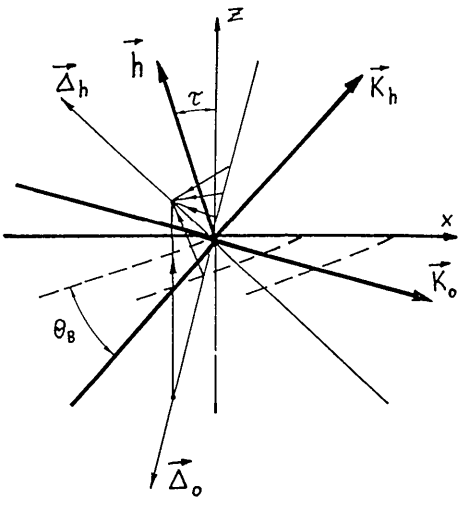

Fig. 3. Scheme describing the TDS contribution to the intensity of a scattered wave.

Here ρ is the density, μ_0 is the absorption coefficient, $\omega_{q\lambda}$ is the phonon frequency and $n_{q\lambda}$ is the number of phonons with a wave vector $\mathbf{q}$ and a branch number λ. $\mathbf{V}_\lambda$ is the polarization vector of the phonons, $\boldsymbol{\eta}=\mathbf{h}/h$, $\hbar$ is Plank's constant.

In the following we shall take into account only acoustic phonons with small values of $\mathbf{q}$. For them

$$n_{q\lambda}\simeq T/\hbar\omega_{q\lambda}, \quad \omega_{q\lambda}=C_\lambda(\mathbf{n})q, \quad \mathbf{n}=\mathbf{q}/q, \tag{5}$$

where T is the temperature in energy units. These phonons alone give the most significant contribution to (4). It is very convenient to introduce the following quantity (Kohn, 1970):

$$C_s^{-2}(\mathbf{n})=\sum\frac{|\boldsymbol{\eta}\mathbf{V}_\lambda|^2}{C_\lambda^2(\mathbf{n})}=\eta^i D_{ik}^{-1}(\mathbf{n})\eta^k, \tag{6}$$

where $D_{ik}(\mathbf{n})$ is a dynamical matrix for the acoustic phonons. In cubic crystals,

$$D_{ik}(\mathbf{n})=\rho^{-1}[\delta_{ik}(an_i^2+b)+(1-\delta_{ik})mn_in_k]. \tag{7}$$

In (7), $a=C_{11}-C_{44}$, $b=C_{44}$, $m=C_{12}+C_{44}$, where C_{11}, C_{12}, C_{44} are elastic constants, δ_{ik} is the Kronecker symbol.

By taking these relations into account one can rewrite (4) in the following form:

$$\frac{\partial^2 P_R^{\mathrm{TDS}}(\alpha)}{\partial\alpha_0\partial\varphi_0}=\frac{TK}{2\mu_0\rho}\frac{\beta}{(1+\beta)}\left(\frac{\lambda r_0 h|F_h|}{2\pi V}\right)^2\frac{C_s^{-2}(\mathbf{n})}{(\psi_m^2+\varphi_0^2+\psi_0^2)}, \tag{8}$$

where $\psi_m=-\alpha\sin 2\theta_b$, $\psi_0=\alpha_0+\alpha\cos 2\theta_b$.

The TDS contribution to the pseudopeak is defined by the angular distribution of the incident radiation. If the incident radiation has a notable divergence, then the specific form of the angular limits is not so important. Let us consider that the incident beam contains all the rays inside a cone with an apex angle Φ. For the integration of (8), we shall use the variable ψ_0 instead of α_0 and neglect the shift of boundaries because $|\alpha|\ll\Phi$. Then in the integral

$$I=\int\mathrm{d}\varphi_0\,\mathrm{d}\psi_0 C_s^{-2}(\mathbf{n})/(\psi_m^2+\varphi_0^2+\psi_0^2), \tag{9}$$

we shall use the polar coordinates $\varphi_0=\rho\cos\xi$ and $\psi_0=\rho\sin\xi$, and the following approximation

$$\begin{aligned}&C_s^{-2}(\mathbf{n})\simeq C_1^{-2}\equiv C_s^{-2}(\mathbf{n}_0), && \rho<\psi_m\\ &C_s^{-2}(\mathbf{n})\simeq C_2^{-2}\equiv(1/2\pi)\int_0^{2\pi}\mathrm{d}\xi\, C_s^{-2}[\mathbf{n}_\infty(\xi)], && \rho>\psi_m,\end{aligned} \tag{10}$$

where $\mathbf{n}_0$ and $\mathbf{n}_\infty(\xi)$ are the directions of $\mathbf{q}$ at $\rho=0$ and $\rho=\infty$, respectively.

As a result, the integral can be easily calculated and for the TDS contribution to the reflection

coefficient we obtain

$$P_R^{\mathrm{TDS}}(\alpha)=\frac{TK}{4\pi\rho\mu_0}\frac{\beta}{(1+\beta)}\left(\frac{\lambda r_0 h|F_h|}{V}\right)^2 \times\left[(C_1^{-2}-C_2^{-2})\frac{\ln 2}{2}+C_2^{-2}\ln\left|\frac{\Phi}{\alpha\sin 2\theta_b}\right|\right]. \quad (11)$$

From (11) it follows that the TDS contribution to the pseudopeak has a weaker logarithmic dependence on α, another dependence on the wavelength (through μ_0) and a different dependence on the order of reflection in comparison with the coherent scattering. In the general case the pseudopeak intensity is defined by the sum of the contributions of $P_R^{\mathrm{coh}}(\alpha)$ and $P_R^{\mathrm{TDS}}(\alpha)$, whereas the main peak is defined only by the coherent contribution to the reflection coefficient of the sample. If we have an asymmetrical reflection ($\beta\neq 1$) for the first crystal and a symmetrical reflection ($\beta=1$) for the sample, the difference between the main peak and the pseudopeak would be observed even in the angular region where the TDS contribution is negligible.

Below we shall consider in more detail the case of symmetrical reflections for all three crystals. In this case, at small values of α, $P_R^{\mathrm{TDS}}\ll P_R^{\mathrm{coh}}$ and the pseudopeak is equal to the main peak $I_{pp}=I_{mp}=P_R^{\mathrm{coh}}$. With increasing α over the value $\alpha=\alpha_{pp}$ ($P_R^{\mathrm{TDS}}=P_R^{\mathrm{coh}}$ at α_{pp}), the intensity of the pseudopeak $I_{pp}=P_R^{\mathrm{TDS}}+P_R^{\mathrm{coh}}$ begins to exceed the intensity of the main peak $I_{mp}=P_R^{\mathrm{coh}}$. At large values of α only P_R^{TDS} remains.

In Fig. 1, one can see the results of the calculations (solid lines) with (1) and (11) for the experiments discussed above. The theoretical and experimental curves for I_{mp} are in very good agreement for both cases of the 400 reflections with Mo $K\alpha$ and Cu $K\alpha$ radiations. By taking the TDS contribution into account, the correspondence of I_{pp} with the experiment improves significantly. In both cases, all the experimental points of I_{pp} are higher than the theoretical curves and the most significant difference is in the range $\alpha\simeq\alpha_{pp}$. The difference decreases with increasing α and a good agreement is observed for $\alpha>1000''$ (see Fig. 1*a*). Note that the calculations were carried out without any fitting parameter.

It is natural to suppose that, besides the considered one-phonon TDS, other mechanisms of scattering, such as a multiphonon diffuse scattering or diffuse scattering by microdefects, contribute to the pseudopeak intensity. The contribution of these processes decreases more sharply at large values of α and has the analogous dependences on α for $\alpha>\alpha_{pp}$. We note that the analysis of the pseudopeak in such cases can be used for studying the diffuse scattering in perfect crystals.

The double-crystal RC $P_R^{2c}(\alpha)$ corresponds to the integral of the TCD curve over the scanning angle $\Delta\theta$. Besides the main peak and the pseudopeak the TCD curve contains also a diffuse contribution. Though a diffuse maximum is not observed the thermal diffuse scattering from the sample contributes to P_R^{2c} by an amount comparable with P_R^{TDS}. Therefore, we can consider that $P_R^{2c}(\alpha)=bP_R^{\mathrm{TDS}}+2P_R^{\mathrm{coh}}$, where b is a numerical coefficient ($1<b<2$). This is the reason that the experimental points of $P_R^{2c}(\alpha)$ are higher than I_{pp} for all the values of α.

As a result of the analysis performed above, we can conclude that the double-crystal rocking curves can be used in the frame of the coherent scattering theory only in the angular range $\alpha<\alpha_{pp}$. From the condition $I_{pp}=I_{mp}$, the value of α_{pp} is easily estimated as the root of the following equation:

$$\frac{Th^4\cos^2\theta_b}{8\pi\rho\mu_0}C_2^{-2}\alpha^2\ln\left|\frac{\Phi}{\alpha\sin 2\theta_b}\right|=1. \quad (12)$$

For our experimental conditions (the angular divergence of the incident beam $\Phi=2°$), the calculated values of α_{pp} were 45″ for Mo $K\alpha$ and 175″ for Cu $K\alpha$ radiation (the correspondent experimental values were 30 and 120″).

As has been noted by Kohn, Prilepsky & Sukhodreva (1984), the high-order reflections are the most informative ones in the structural diagnostics of single-crystal surface layers for two reasons. Firstly, because of the increase in the extinction length the reflection of the layer becomes kinematical. Secondly, there is an increase of the Bragg-angle shift for the reflection by the layer with some lattice strain. On the other hand, according to (12), in this case we have an upper limit on the angular region under consideration. The larger the value of h, the stricter is this limitation. Note that such problems do not arise when the RC is obtained by the TCD method.

4. Crystals with a disturbed surface layer

In this section we present the results of the study of real single crystals with a disturbed surface layer obtained by the DCD and TCD methods. Si crystals of (100) surface orientation were implanted by B^+ ions at 100 keV energy and $10^{19}m^{-2}$ dose and subsequently annealed in an oxygen atmosphere at 1070 K for 10 min (sample 1) and at 1270 K for 40 min (sample 2). The 400 reflection with Cu $K\alpha$ radiation was used. Fig. 4 shows the RCs of the first sample. Curve (1) was measured with the DCD method and curve (2) is the coherent part of the RC obtained by means of the main peak of the TCD curves. The RCs for the second sample (the notations are the same) are shown in Fig. 5. The RCs of a perfect crystal are also shown in these figures for comparison. Curves

(3) and (4) were obtained with the DCD and TCD methods, respectively.

As can be seen in Fig. 4, the shapes of the DCD (1) and TCD (2) curves are similar. Both curves show a set of oscillations at negative angles α, although oscillations are sharper on curve (2). On the whole, curve (2) lies below curve (1). One can see that on average the intensities of the RCs of the sample and the perfect crystal are nearly equal for DCD and TCD

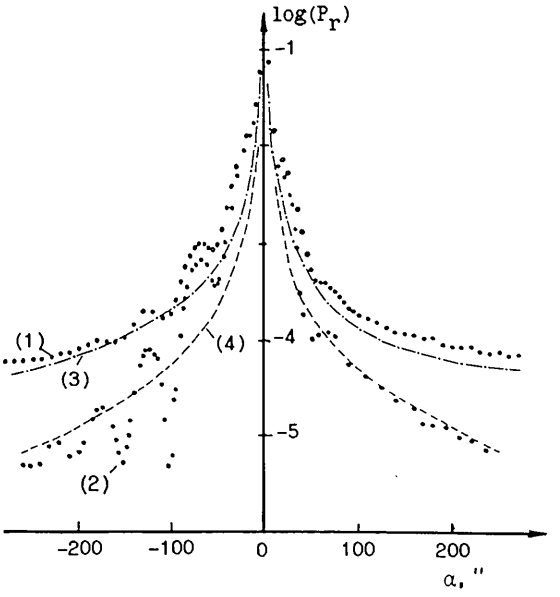

Fig. 4. Experimental rocking curves measured by the DCD [(1), (3)] and TCD [(2), (4)] methods for the first sample [(1), (2)] and for a perfect crystal [(3), (4)].

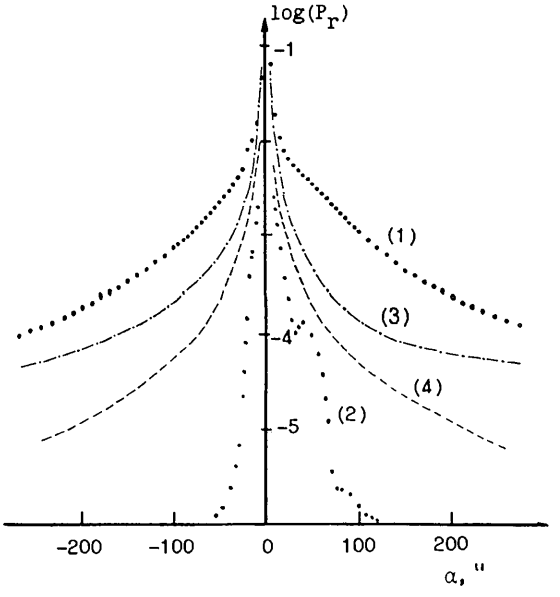

Fig. 5. The same as in Fig. 4 but for the second sample.

methods. The analysis of the TCD curves of the first sample (Fig. 6*b*) shows that there is no noticeable diffuse scattering by microdefects. The difference in the TCD and DCD curves in this case is therefore mainly due to the contribution of the thermal diffuse scattering discussed above.

The situation is quite different for the second sample (Fig. 5). According to electron microscopy studies there is a large density of dislocation loops in the surface layer. The intensity of the DCD curve (1) is significantly higher than the intensity of the DCD curve (3) of the perfect crystal, because of the strong diffuse scattering by the microdefects. One can observe the broad and intense diffuse maximum on the TCD curves of this sample (Fig. 6*c*). The

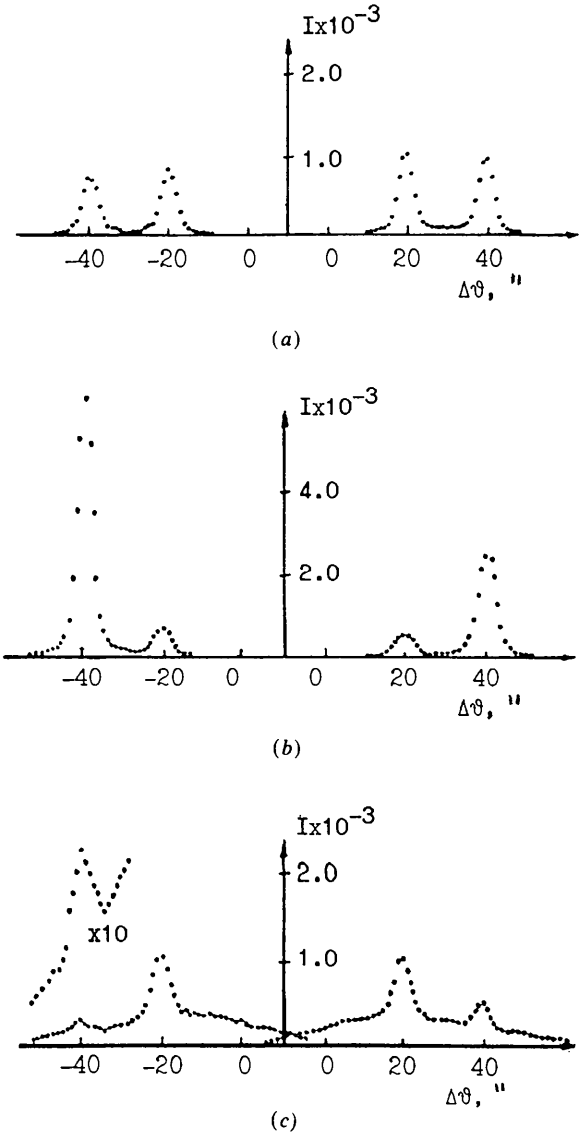

Fig. 6. TCD curves for (*a*) a perfect crystal, (*b*) the first and (*c*) the second samples. I in counts s^{-1}.

integrated values of the main peak were calculated in this case using the assumption that the angular dependence of the diffuse scattering intensity has no peculiarities and can be approximated by the linear function in the angular range of the main peak. The accuracy of the integrated values were estimated as 10–15%. The tails of the TCD curve (2) fall sharply with the increase of $|\alpha|$ and at $\alpha > 0$ one can see a weak maximum which is due to the deformation of the layer by the activated implanted B atoms. The angular position of this maximum allows one to evaluate the average lattice deformation of the layer as $\Delta d/d \simeq -2{\cdot}8 \times 10^{-4}$. It is impossible to obtain quantitative information of this kind using the DCD curve (1). As follows from kinematical theory, a sharp decrease of the TCD curve intensity is connected with the layer lattice disorder, described by the small value of the Debye–Waller factor $\exp(-W)$ (see, for example, Afanasev, Aleksandrov, Imamov, Lomov & Zavyalova, 1984).

Therefore, for sample (2) the RC measured by the DCD method is the angular dependence of the sum of the intensities of the strong diffuse waves and the extremely weak coherent wave. The TCD method allows one to measure a weak coherent component on the background of an intense diffuse scattering, which can be two or three orders of magnitude higher than the coherent one (Kazimirov, Kovalchuk & Kohn, 1987).

The authors thank S. Yu. Shiryaev for supplying the samples and for useful discussions.

References

AFANASEV, A. M., ALEKSANDROV, P. A., IMAMOV, R. M., LOMOV, A. A. & ZAVYALOVA, A. A. (1984). *Acta Cryst.* A**40**, 352–355.

AFANASEV, A. M., KAGAN, Y. M. & CHUKOVSKII, F. N. (1968). *Phys. Status Solidi*, **28**, 287–294.

AFANASEV, A. M., KOVALCHUK, M. V., KOVEV, E. K. & KOHN, V. G. (1977). *Phys. Status Solidi A*, **42**, 415–422.

BURGEAT, J. & TAUPIN, D. (1968). *Acta Cryst.* A**24**, 99–102.

CEMBALI, F., SERVIDORI, M., GABILLI, E. & LOTTI, R. (1985). *Phys. Status Solidi A*, **87**, 225.

CEMBALI, F., SERVIDORI, M., SOLMI, S., SOUREK, Z., WINTER, U. & ZAUMSEIL, P. (1986). *Phys. Status Solidi A*, **98**, 511–516.

FUKUHARA, A. & TAKANO, Y. (1977). *Acta Cryst.* A**33**, 137–142.

IIDA, A. & KOHRA, K. (1979). *Phys. Status Solidi A*, **51**, 533–542.

KAZIMIROV, A. YU., KOVALCHUK, M. V. & KOHN, F. G. (1987). *Metallofizica*, **9**, 54–58.

KOHN, V. G. (1970). *Sov. Phys. Crystallogr.* **15**, 14–17.

KOHN, V. G., KOVALCHUK, M. V., IMAMOV, R. M. & LOBANOVICH, E. F. (1981). *Phys. Status Solidi A*, **64**, 435–442.

KOHN, V. G., PRILEPSKY, M. V. & SUKHODREVA, I. M. (1984). *Poverkhn.* pp. 122–128.

KYUTT, R. N., PETRASHEN, P. V. & SOROKIN, L. M. (1980). *Phys. Status Solidi A*, **60**, 381–389.

PINSKER, Z. G. (1978). *Dynamical Scattering of X-rays in Crystals.* Heidelberg, New York: Springer-Verlag.

SPERIOSU, V. S., GLASS, H. L. & KOBAYASHI, T. (1979). *Appl. Phys. Lett.* **34**, 539–542.

ZAUMSEIL, P. (1985). *Phys. Status Solidi A*, **91**, 31.

ZAUMSEIL, P., WINTER, U., CEMBALI, F., SERVIDORI, M. & SOUREK, Z. (1987). *Phys. Status Solidi A*, **100**, 95–104.

Acta Cryst. (1990). A**46**, 649–656

X-ray Standing Waves in the Laue Case – Location of Impurity Atoms

BY A. YU. KAZIMIROV AND M. V. KOVALCHUK

A. V. Shubnikov Institute of Crystallography of the Academy of Sciences of the USSR, Leninsky Prospect 59, *Moscow* 117333, *USSR*

AND V. G. KOHN

I. V. Kurchatov Institute of Atomic Energy, Kurchatov Square 46, *Moscow* 123182, *USSR*

(*Received* 17 *February* 1989; *accepted* 12 *February* 1990)

Abstract

Impurity-atom fluorescence excited by X-ray standing waves in the Laue case of X-ray diffraction has been investigated experimentally and theoretically. Possibilities for location of impurity atoms in the bulk and the surface layer of single crystals are discussed. The experiments were carried out on silicon crystals of different thicknesses doped with germanium. The general approach for calculation of the fluorescence-yield angular curves has been developed. In the case of the uniform distribution of impurity atoms in the bulk of a crystal and also in the case of the kinematical X-ray diffraction on a thin surface layer, analytical expressions can be used.

1. Introduction

According to dynamical theory, during X-ray diffraction in a nearly perfect crystal X-ray standing waves (XSW) are generated. The period of this wave is equal to or smaller by an integer than the interplanar

0108-7673/90/080649-08$03.00